Brief Communications

Amyloid-β_{1-42} Slows Clearance of Synaptically Released Glutamate by Mislocalizing Astrocytic GLT-1

Annalisa Scimemi,[1]* James S. Meabon,[2,6]* Randall L. Woltjer,[7] Jane M. Sullivan,[5] Jeffrey S. Diamond,[1] and David G. Cook[3,4,6]

[1]Synaptic Physiology Section, National Institute of Neurological Disorders and Stroke, National Institutes of Health, Bethesda, Maryland 20892, Departments of [2]Psychiatry, [3]Medicine, and [4]Pharmacology, University of Washington, Seattle, Washington 98108, [5]Department of Physiology and Biophysics, University of Washington, Seattle, Washington 98195, [6]Geriatric Research Education and Clinical Center, Veterans Affairs Medical Center (VA Puget Sound Health Care System), Seattle, Washington 98108, and [7]Department of Pathology, Oregon Health & Sciences University, Portland, Oregon 97239

GLT-1, the major glutamate transporter in the adult brain, is abundantly expressed in astrocytic processes enveloping synapses. By limiting glutamate escape into the surrounding neuropil, GLT-1 preserves the spatial specificity of synaptic signaling. Here we show that the amyloid-β peptide Aβ_{1-42} markedly prolongs the extracellular lifetime of synaptically released glutamate by reducing GLT-1 surface expression in mouse astrocytes and that this effect is prevented by the vitamin E derivative Trolox. These findings indicate that astrocytic glutamate transporter dysfunction may play an important role in the pathogenesis of Alzheimer's disease and suggest possible mechanisms by which several current treatment strategies could protect against the disease.

Introduction

Glutamate transporters bind and remove glutamate from the extracellular space. In adult hippocampus this task is performed primarily by two astrocytic transporter subtypes: GLT-1 and GLAST (homologous to human excitatory amino acid transporters EAAT1 and EAAT2, respectively) (Kanai and Hediger, 1992). The activity of these transporters is crucial to ensure pathway specificity of synaptic transmission and plasticity (Diamond and Jahr, 1997; Tsvetkov et al., 2004), prevent glutamate-induced excitotoxicity (Tanaka et al., 1997), regulate ammonia detoxification (Felipo and Butterworth, 2002), and modulate activity-dependent glucose utilization (Voutsinos-Porche et al., 2003). Several studies indicate that glutamate transporters are impaired in Alzheimer's disease (AD) (Masliah et al., 1996; Lauderback et al., 2001; Jacob et al., 2007). GLT-1 loss and reduced detergent solubility of the remaining GLT-1 occur in early prodromal AD and become more prominent with increasing cognitive impairment (Woltjer et al., 2010). Partial GLT-1 loss in an animal model of AD also provokes early-occurring cognitive deficits (Mookherjee et al., 2011), suggesting that GLT-1 loss is capable of driving cognitive impairment in the context of Aβ-related neuropathology. Whether Aβ-related pathogenic processes have a functional impact on the rate at which astrocytes remove endogenous, synaptically released glutamate is unknown. Here we show that Aβ_{1-42} induces rapid GLT-1 mislocalization and internalization in astrocytes, which leads to a marked reduction in the rate at which astrocytes clear up synaptically released glutamate from the extracellular space. Importantly, we show that pretreatment with the vitamin E derivative, Trolox, prevents the effects of Aβ_{1-42} on GLT-1 and astrocytic glutamate clearance.

Materials and Methods

Electrophysiology and data analysis. P14–P21 C57BL/6 mice of either sex were deeply anesthetized with halothane and decapitated, in accordance with the NINDS and Veterans Affairs Animal Use Committees guidelines. Transverse hippocampal slices (250 μm thick) were obtained with a vibrating blade microtome (VT1000S, Leica Microsystems). The slicing solution, kept at 4°C and continuously bubbled with a mixture of 95% O_2-5% CO_2, contained the following (in mM): 119 NaCl, 2.5 KCl, 0.5 $CaCl_2$, 1.3 $MgSO_4 \cdot 7H_2O$, 4 $MgCl_2$, 26.2 $NaHCO_3$, 1 NaH_2PO_4, 22 glucose, 320 mOsm, pH 7.4. After cutting, slices were kept in this solution in a submersion chamber at 34°C for 30 min, and at room temperature thereafter for up to 5 h. Recording solution contained the following (in mM): 119 NaCl, 2.5 KCl, 2.5 $CaCl_2$, 1.3 $MgSO_4 \cdot 7H_2O$, 26.2 $NaHCO_3$, 1 $NaHPO_4$, 22 glucose, 300 mOsm, pH 7.4, saturated with 95% O_2-5% CO_2. All recordings were performed at 34–36°C. The following drugs were routinely added to the artificial CSF to block AMPA, NMDA, and metabotropic glutamate receptors, $GABA_A$, $GABA_B$, and adenosine receptors: 2,3-dioxo-6-nitro-1,2,3,4-tetrahydrobenzoquinoxaline-7-sulfonamide disodium salt (NBQX; 10 μM), (*R*,*S*)-3-(2-carboxypiperazin-4-yl)-propyl-1-phosphonic acid (CPP; 10 μM), 2-[(1*S*,2*S*)-2-carboxycyclopropyl]-3-(9*H*-xanthen-9-yl)-D-alanine (LY341495; 1 μM), (*R*,*S*)-α-methylserine-*O*-phosphate (MSOP; 100 μM), picrotoxin (100 μM), 3-[[(3,4-dichlorophenyl)methyl]amino]propyl]diethoxymethyl)phosphinic acid (CGP52432; 5 μM), 8-cyclopentyl-1,3-dipropylxanthine (DPCPX; 1 μM). Astrocytes in CA1 stratum radiatum were identified under IR-DIC using an upright microscope (Axioskop 2FS, Zeiss). Electrophysiological recordings were made with 2.5–3.0 MΩ patch

Received Nov. 1, 2012; revised Jan. 11, 2013; accepted Feb. 5, 2013.

Author contributions: A.S., J.S.M., and D.G.C. designed research; A.S. and J.S.M. performed research; R.L.W., and J.M.S. contributed unpublished reagents/analytic tools; A.S., J.S.M., and D.G.C. analyzed data; A.S., J.S.M., J.S.D., and D.G.C. wrote the paper.

This work was supported by the Veteran's Affairs Office of Research and Development Medical Research Service (D.G.C.), NIH (Grants T32 AG000258, J.S.M.; and RO1 NS055804, J.M.S.), and NINDS Intramural Research Program (Grant NS002986, J.S.D.). We thank Mike Ahlquist, Ping Zhu, and Ning Li for excellent technical assistance.

The authors declare no competing financial interests.

*A.S. and J.S.M. contributed equally to this report.

Correspondence should be addressed to Dr. David G. Cook, VA Medical Center, GRECC, 1660 S. Columbian Way, Seattle, WA 98108. E-mail: dgcook@u.washington.edu.

DOI:10.1523/JNEUROSCI.5274-12.2013

 0270-6474/13/335312-07$15.00/0

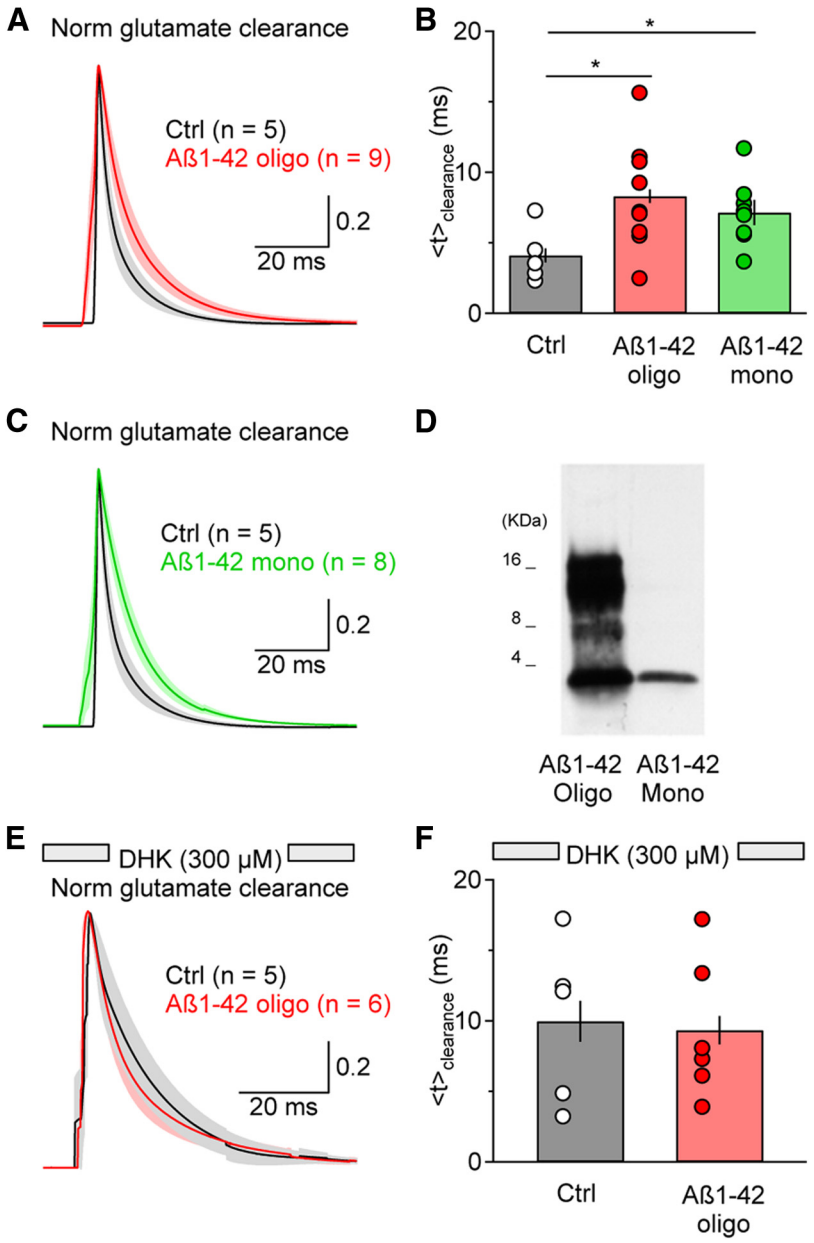

Figure 1. Aβ_{1-42} prolongs the time course of glutamate clearance via GLT-1. ***A***, Deconvolution-derived time course of glutamate clearance in Control (black) and oligomerized Aβ_{1-42} (A$\beta_{1-42\ oligo}$; red). ***B***, Summary graph of the estimated centroid of glutamate clearance ($\langle t \rangle_{clearance}$) in Control, A$\beta_{1-42\ oligo}$, and monomeric A$\beta_{1-42}$ (A$\beta_{1-42\ mono}$). A$\beta_{1-42\ oligo}$ and A$\beta_{1-42\ mono}$ significantly prolonged the time course of glutamate clearance by astrocytes. ***C***, Deconvolution-derived time course of glutamate clearance in Control (black) and A$\beta_{1-42\ mono}$ (green). ***D***, Western blot using anti-Aβ 6E10 antibody shows pattern of oligomeric (Oligo) and monomeric (Mono) Aβ_{1-42}. ***E***, Deconvolution-derived time course of glutamate clearance in DHK (300 μM), in the absence (Ctrl, black) or presence of A$\beta_{1-42\ oligo}$ (red). ***F***, Summary graph of the estimated $\langle t \rangle_{clearance}$ in the conditions described in ***E***. In the presence of DHK, Aβ_{1-42} does not change the time course of glutamate clearance by astrocytes. Shaded areas in ***A***, ***C***, and ***E*** represent SEM.

pipettes filled with (in mM): 120 $CsCH_3SO_3$, 10 EGTA, 20 HEPES, 2 MgATP, 0.2 NaGTP, 5 QX-314Br, biocytin (0.4% w/v) 290 mOsm, pH 7.2. After each recording, the slices were fixed overnight in 4% paraformaldehyde and stored in PBS for histochemical processing. Transporter currents were evoked by applying 50 μs, constant voltage, electrical pulses to stratum radiatum through bipolar stainless steel electrodes (Frederick Haer Company) located ~100 μm away from their cell body. Single and paired pulses, 100 ms apart, were delivered every 10 s. Reagents were from Sigma and Tocris Bioscience. Currents were filtered at 2 kHz, digitized at 5 kHz, and acquired with custom-made software (A.S., J.S.D) written in IgorPro (Wavemetrics). Data analysis was performed within the IgorPro environment using custom-made software (A.S.). The analysis was performed on transporter currents isolated by subtracting the average response to single pulse stimulations from that evoked by paired stimuli (Diamond, 2005; Scimemi et al., 2009). The time course of the glutamate clearance waveform ($F(t)$) was measured as the centroid $\langle t \rangle$, where:

$$< t > \ = \frac{\int F(t) t dt}{\int F(t) dt}.$$

Changes in $\langle t \rangle$ reflect changes in the rising and decaying phase of glutamate clearance.

Cultured astrocytes. C57BL/6;129Sv mice of either sex were used in accord with protocols approved by the University of Washington Animal Care and Use Committee. Neocortex from neonatal mice was digested with papain and grown in MEM supplemented with 5% fetal calf serum, GlutaMAX, 20 mM glucose, and penicillin/streptomycin (Life Technologies). Confluent astrocyte cultures were purified by shaking, replated, grown 7–10 d, and treated with 0.15 mM dibutyryl-cAMP (Sigma), 10 μM Ara-C, 3% FBS, GlutaMAX in MEM for 96 h to increase GLT-1 expression (Swanson et al., 1997). Medium was replaced with normal medium for 6 h before treatment with Aβ_{1-42} (30 min, 37°C). While chilled at 4°C, astrocytes were treated with Pierce EZ-Link Sulfo-NHS-SS-Biotin (Thermo Scientific) according to the manufacturer's protocol.

Aβ oligomerization and treatment solutions. Synthetic human Aβ_{1-42} peptide (CPC Scientific) oligomerization was performed as described previously (Stine et al., 2003) and confirmed using Western blots (Fig. 1*D*) from 16.5% tricine-gel (Bio-Rad) SDS polyacrylamide gels immunoblotted with 6E10 antibodies (Covance). Control condition did not contain Aβ_{1-42} peptide but was otherwise identically prepared. As a final step, 0.1% (w/v) BSA (used as a carrier protein) was added to each aliquot and mixed before storage. Equal volumes of Control and Aβ_{1-42} aliquots were diluted into either electrophysiology solutions or astrocyte medium (depending on the experiment) to a final concentration of 500 nM Aβ_{1-42} and 0.0005% BSA protein carrier.

Confocal microscopy. Slices containing biocytin-filled astrocytes were fixed in 4% paraformaldehyde and permeabilized with 0.25% Triton X-100/PBS. Biocytin and GLT-1 were visualized with streptavidin Alexa Fluor 488 and anti-rabbit/Alexa Fluor 568 (Life Technologies), respectively. Slices were imaged on a Nikon A1R confocal microscope. Each stack contained 15–30 images acquired at 0.25 μm intervals. Final figures were prepared using Adobe Photoshop, where only linear brightness and contrast adjustments were performed identically on Aβ_{1-42}-treated and control slice images.

Biochemistry. Protein lysates from slices and cultured astrocytes were prepared using 1% Triton X-100 buffer [in mM: 20 Tris, 1 EDTA, 0.5 EGTA, 250 sucrose, Protease Inhibitor Cocktail (EMD Millipore)]. Lysate protein concentrations were determined by bicinchoninic acid assay (Thermo Scientific). Lysates were electrophoresed on 4–20% SDS polyacrylamide gels (Bio-Rad) and transferred onto Immobilon-P membranes (Millipore). Antibodies recognizing GLT-1 (Millipore) and AB12

(gift from Dr. David Pow, RMIT University of Melbourne, Australia) (Mookherjee et al., 2011), GLAST (Cell Signaling Technology), and EAAC1 (Alpha Diagnostics) were used. Pyruvate kinase (Rockland) and Sypro Ruby protein blot stain (Life Technologies; conducted before blocking as per manufacturer's protocol) were used as controls for soluble and insoluble protein fractions, respectively. Bands were visualized with ECL-Plus (GE Healthcare). Optical densitometry measurements were performed with ImageJ (NIH), and protein bands were normalized with respect to their respective protein load signals (pyruvate kinase for Triton X-100-soluble protein fractions and Sypro Ruby for detergent-insoluble protein fractions) and normalized against identically determined average control values. Biotinylated cell surface proteins were pulled down from 10 μg of whole-cell Triton X-100 lysates using Neutravidin beads (Thermo Scientific). Because intracellular GLT-1 expression predominates in purified cultured astrocytes, pull-downs were run alongside 1 μg of their corresponding lysates to avoid saturating the linear range of the imaging device (GE Healthcare ImageQuant LAS/4000). The GLT-1 detergent insolubility measures were performed on acute brain slices prepared and stored as described for the electrophysiological experiments. Slices were treated for 30 min with vehicle control or 500 nM $A\beta_{1-42,}$ with or without a 1 h pretreatment with 100 μM Trolox (Sigma). Slices were extracted three times (1 h each) in 1%Triton X-100 lysis buffer and clarified by high-speed centrifugation (100,000 $\times$ *g*) to separate the Triton X-100-soluble supernatant and Triton X-100-insoluble pellet. For ubiquitin/GLT-1 immunoprecipitation/Western blots, 100 μg samples (obtained from the first of three serial Triton X-100 protein extractions prepared during the GLT-1 detergent insolubility experiments; see Fig. 3) were immunoprecipitated with anti-Ubiquitin P4D1 monoclonal antibody (Santa Cruz Biotechnology) and Protein G Agarose beads (Life Technologies).

Statistical analysis. Student's *t* tests and ANOVA were performed as appropriate (Winer et al., 1991) using SPSS software (IBM).

Results

We recorded synaptically activated transporter currents (STCs) from astrocytes in acute mouse hippocampal slices, before and after applying a subsaturating concentration of the broad-spectrum glutamate transporter antagonist TBOA (DL-*threo*-β-benzyloxyaspartic acid; 10 μM). By monitoring the effect of TBOA on the STCs, we estimated the time course of synaptically released glutamate clearance from astrocytes as previously described (Diamond, 2005; Scimemi et al., 2009) (Fig. 1*A*; Materials and Methods). To test whether $A\beta_{1-42}$ alters glutamate clearance in astrocytes, we applied this analytical approach to STCs recorded from astrocytes in control slices (i.e., slices perfused with 0.0005% bovine serum albumin) and in slices treated with monomeric or oligomeric $A\beta_{1-42}$ (500 nM) and 0.0005% bovine serum albumin protein carrier. TBOA reduced the STC amplitude to the same extent in all conditions (normalized STC amplitude: Control 0.25 $\pm$ 0.08, $n = 5$; $A\beta_{1-42\ \mathrm{oligo}}$ 0.27 $\pm$ 0.04, $n = 9$; $A\beta_{\mathrm{mono}}$ 0.32 $\pm$ 0.08, $n = 8$; $p_{\mathrm{Control\text{-}A\beta1-42\ oligo}} = 0.80$, $p_{\mathrm{Control\text{-}A\beta1-42\ mono}} = 0.56$). However, as shown in Figure 1*A–C*, the time course of glutamate clearance (expressed as the centroid, $\langle t \rangle$) was significantly slower in slices treated with oligomerized or monomeric $A\beta_{1-42}$ ($\langle t \rangle_{\mathrm{clearance\ Control}} = 4.1 \pm 0.5$ ms, $n = 5$; $\langle t \rangle_{\mathrm{clearance\ A\beta1-42\ oligo}} = 8.3 \pm 0.5$ ms, $n = 9$, $^{*}p_{\mathrm{Control\text{-}A\beta1-42\ oligo}} = 0.044$; $\langle t \rangle_{\mathrm{clearance\ A\beta1-42\ mono}} = 7.1 \pm 0.9$ ms, $n = 8$, $^{*}p_{\mathrm{Control\text{-}A\beta1-42\ mono}} = 0.036$). These results suggest that $A\beta_{1-42}$ rapidly impairs astrocytic glutamate transport. Because there was no difference between the effects of monomeric or oligomeric $A\beta_{1-42}$ preparations on glutamate clearance ($p = 0.47$), in all remaining experiments we used oligomerized $A\beta_{1-42}$ preparations (hereafter referred to as $A\beta_{1-42}$), as they contained a mixture of monomeric and higher-order Aβ species potentially emulating a spectrum of synthetic $A\beta_{1-42}$ conformers similar to those found in AD patients (Fig. 1*D*; Materials and Methods).

The slower time course of glutamate clearance from astrocytes treated with $A\beta_{1-42}$ could be mediated by one or more astrocytic glutamate transporter subtypes. We asked whether GLT-1 and/or GLAST mediated the effects of $A\beta_{1-42}$. Under our experimental conditions, GLAST contributes ~1/3 of the total astrocytic glutamate transport, with the rest contributed by GLT-1 (Scimemi et al., 2009). We found that the specific GLT-1 inhibitor DHK (dihydrokainate; 300 μM) prolonged the time course of glutamate clearance ($\langle t \rangle_{\mathrm{clearance\ DHK}} = 10.0 \pm 2.6$ ms, $n = 5$; Fig. 1*E,F*), in agreement with previous reports (Diamond, 2005; Scimemi et al., 2009). The time course of glutamate clearance in the presence of DHK was comparable to that observed in slices treated with $A\beta_{1-42}$ ($p = 0.53$) and, in the presence of DHK, $A\beta_{1-42}$ failed to prolong glutamate clearance ($\langle t \rangle_{\mathrm{clearance\ DHK+A\beta1-42}} = 9.3 \pm 2.0$ ms, $n = 6$; $p = 0.85$). These results indicate that the $A\beta_{1-42}$-induced slowing of glutamate clearance could be accounted for entirely by effects on glutamate uptake by GLT-1.

One possible mechanism underlying the effects of $A\beta_{1-42}$ on astrocyte-mediated glutamate clearance is reduced membrane expression of GLT-1. To test this hypothesis, we used confocal microscopy to image biocytin-filled astrocytes and GLT-1. Normally GLT-1 is expressed only at the plasma membrane of astrocytes (Chaudhry et al., 1995). In keeping with this, GLT-1 immunoreactivity (red) appeared to localize primarily at or near the cell surface of control astrocytes filled with biocytin (green) (Fig. 2*A*, top row; single *z*-plane image showing one of 19 biocytin-labeled astrocytes examined). In contrast, GLT-1 immunoreactivity appeared to colocalize extensively with the biocytin signal in the cytoplasm of $A\beta_{1-42}$-treated astrocytes (Fig. 2*A*, bottom row; single *z*-plane image showing one of 9 biocytin-labeled astrocytes examined). This finding suggests that $A\beta_{1-42}$ alters GLT-1 expression at or near the astrocytic plasma membrane.

To test quantitatively whether $A\beta_{1-42}$ induced GLT-1 internalization, we turned from acute hippocampal slices to cultured astrocytes, which are better suited for measuring cell-surface protein expression via cell-surface biotinylation. Repeating the $A\beta_{1-42}$ treatment protocol on cultured astrocytes (i.e., 30 min application of $A\beta_{1-42}$, 500 nM), we found that GLT-1 cell surface expression was significantly reduced by $A\beta_{1-42}$ treatment (mean optical density: $A\beta_{1-42} = 0.67 \pm 0.07$, $n = 8$; Control = 1.0 ± 0.09, $n = 8$, $p = 0.01$; Fig. 2*B,E*), while GLAST cell surface expression was not altered ($A\beta_{1-42} = 1.04 \pm 0.19$, $n = 8$; Control = 1.0 ± 0.19, $n = 8$, $p = 0.86$, Fig. 2*D,E*). Total protein levels of GLT-1 and GLAST in cultured astrocytes were not significantly altered by $A\beta_{1-42}$ exposure (total mean GLT-1: $A\beta_{1-42} = 0.99 \pm 0.11$, $n = 8$; Control = 1.0 ± 0.04, $n = 8$, $p = 0.933$; total mean GLAST: 0.90 ± 0.11, $n = 8$, Control = 1.0 ± 0.08, $n = 8$, $p = 0.50$; Fig. 2*C,E*). Similarly, in hippocampal slices, the total levels of GLT-1, GLAST, and the neuronal glutamate transporter EAAC1 were unaffected by $A\beta_{1-42}$ treatment (GLT-1: Control = 1.0 ± 0.07, $n = 6$, $A\beta_{1-42} = 0.86 \pm 0.08$, $n = 6$; $p = 0.20$; GLAST: Control = 1.0 ± 0.11, $n = 6$, $A\beta_{1-42} = 0.77 \pm 0.08$, $n = 6$; $p = 0.12$; EAAC1: Control = 1.0 ± 0.11, $n = 6$, $A\beta_{1-42} = 0.86 \pm 0.10$, $n = 6$; $p = 0.39$; Western blots not shown). Together, these data indicate that $A\beta_{1-42}$ slowed clearance of synaptically released glutamate by disrupting GLT-1 localization at/near the astrocytic plasma membrane.

Previous work showed that $A\beta_{1-42}$ oxidatively damages GLT-1 (Guo and Mattson, 2000; Lauderback et al., 2001) and that oxidative stress promotes formation of aberrant high molecular weight GLT-1 complexes that are insoluble in detergents such as Triton X-100 (Haugeto et al., 1996; Trotti et al., 1997, 1998).

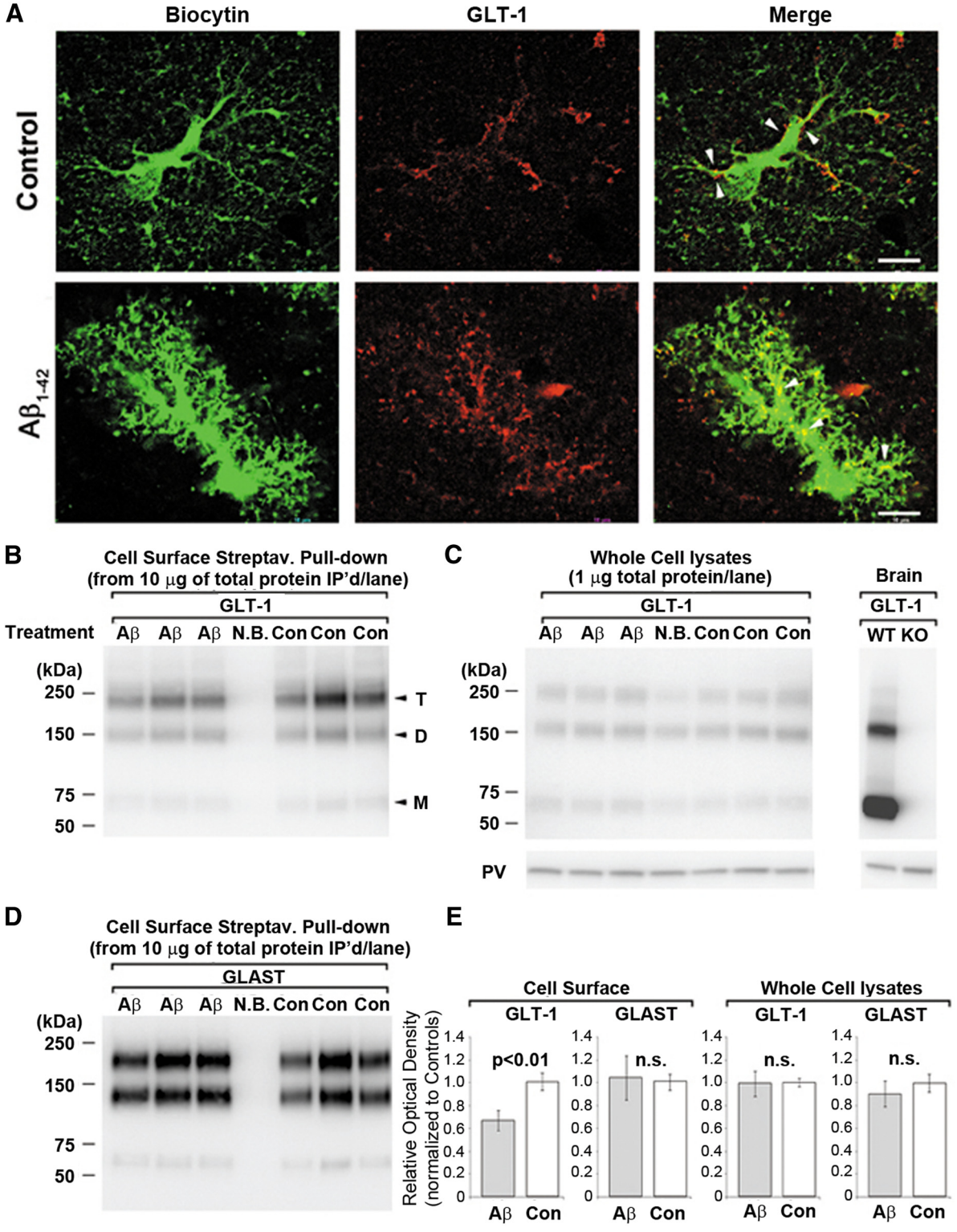

Figure 2. Aβ_{1-42} reduces GLT-1 cell surface expression. ***A***, In hippocampal slices under control conditions, GLT-1 (red) was localized at or near the plasma membrane (arrowheads) of biocytin-filled astrocyte (top). In Aβ_{1-42}-treated astrocytes (bottom) GLT-1 colocalized with green cytosolic biocytin staining (yellow in merged panel, arrowheads). ***B***, Under the same conditions used in slices, cultured astrocytes were exposed to Aβ_{1-42} and cell-surface protein biotinylated to quantify GLT-1 cell-surface expression. Aβ_{1-42} treatment reduced cell-surface expression of GLT-1 in cultured primary astrocytes compared with Control (Con) when assayed with pull-down of biotinylated cell-surface proteins using strepavidin beads from 10 μg of whole-cell protein lysates. ***C***, Total GLT-1 expression from the same whole-cell protein lysates (1 μg total protein/lane) was not changed by treatment (left). Right panel demonstrates GLT-1 antibody specificity against WT versus GLT-1 KO mouse brain lysate. Pyruvate kinase (PK) was used as a protein load control. ***D***, Re-probing pull-downs for GLAST showed that cell-surface GLAST expression was not altered by Aβ_{1-42}. ***E***, Summary of cell-surface pull-downs and whole-cell lysate expression levels of GLT-1 and GLAST from three independent experiments performed each time in triplicate (three lanes for each treatment per gel). NB, Nonbiotinylated sample; T, trimer; D, dimer; M, monomer. Scale bars, 10 μm.

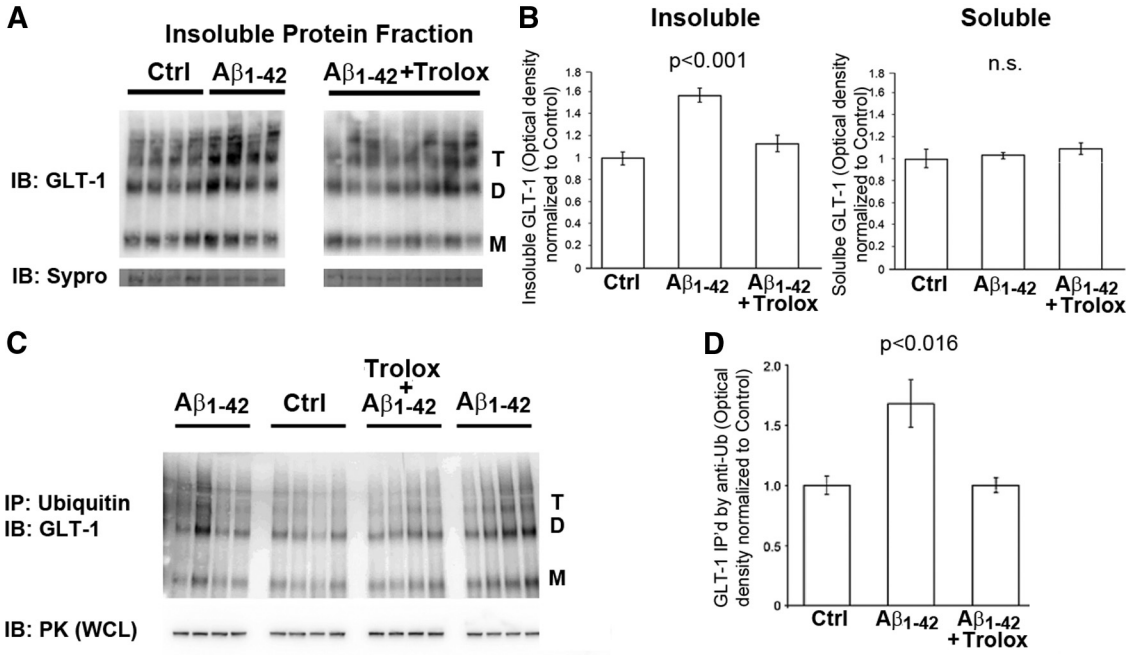

Figure 3. Pretreating hippocampal slices with Trolox rescues $A\beta_{1-42}$-induced GLT-1 Triton X-100 detergent-insolubility and ubiquitination. ***A***, Representative Western blots show GLT-1 levels in protein lysates first subjected to three serial 1% Triton X-100 extractions to remove Triton X-100-soluble proteins. $A\beta_{1-42}$ increased detergent-insoluble GLT-1 levels compared with control slices. Trolox reduced GLT-1 detergent-insolubility to control levels. Prestaining with Sypro confirmed equivalent protein loading among lanes. ***B***, $A\beta_{1-42}$ increased Triton X-100-insoluble GLT-1 (left) and was rescued by Trolox pretreatment (Ctrl, $A\beta_{1-42}$, and $A\beta_{1-42}$ pretreated 1 h before and during 30 min $A\beta_{1-42}$ treatment; $n = 9$, 50, and 18, respectively; $F_{(2,74)} = 13.605$, $p < 0.001$; and $A\beta_{1-42}$ versus {Ctrl and $A\beta_{1-42}$+Trolox}, $p < 0.001$). There were no significant differences in Triton X-100-soluble GLT-1. ***C***, Immunoprecipitation/Immunoblots (IP/IB) of these same lysates demonstrate increased levels of ubiquitinated GLT-1 in $A\beta_{1-42}$-treated slices compared with control and $A\beta_{1-42}$+Trolox-pretreated slices. Pyruvate kinase (PK) from whole-cell lysates (WCL; 1 μg/lane) was used as a protein load control. T, Trimer; D, dimer; M, monomer. ***D***, Summary histograms show quantification of ubiquitinated GLT-1 levels from hippocampal slices (Ctrl, $A\beta_{1-42}$, and $A\beta_{1-42}$ pretreated 1 h before and during 30 min Aβ treatment; $n = 6$, 10, and 4, respectively; $F_{(2,17)} = 5.354$, $p < 0.016$; and $A\beta_{1-42}$ group versus {Ctrl and $A\beta_{1-42}$+Trolox}, $p < 0.005$.

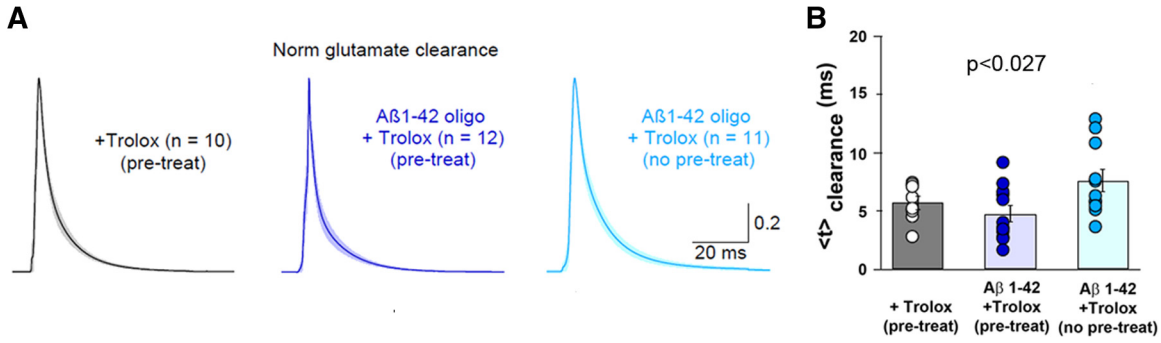

Figure 4. Pretreating hippocampal slices with Trolox prevents $A\beta_{1-42}$-induced slowing of synaptic glutamate clearance. ***A***, Deconvolution-derived time course of glutamate clearance recorded from astrocytes in hippocampal slices pretreated with Trolox (100 μM; black), pretreated with Trolox and exposed to $A\beta_{1-42}$ (blue), or exposed to both Trolox and $A\beta_{1-42}$ (light blue). Shaded areas represent SEM. ***B***, Summary graph of the estimated centroid of glutamate clearance ($\langle t \rangle_{clearance}$) in each of the conditions described in *A*. Trolox pretreatment prevented $A\beta_{1-42}$ from slowing clearance of synaptically released glutamate. Without Trolox pretreatment, $A\beta_{1-42}$ slowed down astrocytic glutamate clearance (Trolox pretreat, $n = 10$; $A\beta_{1-42}$+Trolox pretreat, $n = 12$; $A\beta_{1-42}$+Trolox no pretreat, $n = 11$; overall ANOVA $F_{(2,30)} = 4.086$, $p < 0.027$.

These findings raise the possibility that $A\beta_{1-42}$ alters GLT-1 surface expression and astrocytic glutamate clearance by activating oxidative stress responses. To test this hypothesis we assessed the ability of $A\beta_{1-42}$ to induce GLT-1 detergent insolubility in hippocampal slices and tested whether Trolox, a highly water-soluble derivative of the anti-oxidant, vitamin E (Quintanilla et al., 2005), was capable of blocking the effects of $A\beta_{1-42}$ on GLT-1.

We found that GLT-1 levels in the Triton X-100-insoluble protein fraction (i.e., proteins remaining as a pellet after three serial Triton X-100 extractions) from $A\beta_{1-42}$-treated slices were significantly elevated compared with controls (Fig. 3*A*,*B*, left). By contrast, $A\beta_{1-42}$ treatment had no effect on GLT-1 levels in the detergent-soluble protein fraction (Fig. 3*B*, right). Normal levels of detergent-insoluble GLT-1 were restored by pretreating the slices with Trolox (100 μM; 1 h preincubation plus the 30 min $A\beta_{1-42}$ exposure period) ($F_{(2,74)} = 13.605$, $p < 0.001$; Fig. 3*B*, left).

Aberrant post-translational modifications are closely associated with detergent-insoluble protein aggregation in AD (Woltjer et al., 2005). In keeping with this, $A\beta_{1-42}$ promotes pathologic oxidative stress-induced covalent modifications of numerous proteins and lipid moieties (Sultana et al., 2006). Intriguingly, recent studies found that ubiquitination of GLT-1 causes it to internalize from the cell surface of astrocytes (Martínez-Villarreal et al., 2012). These findings raised the question whether oxidative stress elicited by $A\beta_{1-42}$ exposure induces GLT-1 ubiquitination.

To address this possibility, hippocampal slices were treated as described above. Ubiquitinated proteins were immunoprecipitated with anti-Ubiquitin antibodies and Western blotted for GLT-1. The results in Figure 3, *C* and *D*, show that $A\beta_{1-42}$ treatment significantly increased GLT-1 ubiquitination and that this effect was blocked by Trolox pretreatment ($F_{(2,17)} = 5.354$, $p < 0.016$).

To address the functional significance of Trolox pretreatment on GLT-1 function in astrocytes, we again recorded STCs from astrocytes in hippocampal slices (Fig. 4). We first confirmed that the Trolox pretreatment on its own did not change the time course of glutamate clearance compared with control conditions ($\langle t \rangle_{\text{Trolox}} = 5.8 \pm 0.5$ ms, $n = 10$ $p = 0.09$). Notably, the time course of glutamate clearance was not prolonged by $A\beta_{1-42}$ in slices pretreated with Trolox ($\langle t \rangle_{A\beta 1-42+\text{Trolox pretreat}} = 4.7 \pm 0.7$ ms, $n = 12$,). By contrast, the time course of glutamate clearance was still prolonged by $A\beta_{1-42}$ and Trolox in slices not pretreated with Trolox ($\langle t \rangle_{A\beta 1-42+\text{Trolox no pretreat}} = 7.6 \pm 0.9$ ms, $n = 11$) ($F_{(2,30)} = 4.086$, $p < 0.027$). These results suggest that the ability of Trolox to prevent the effects of $A\beta_{1-42}$ is not due to direct molecular interactions between Trolox and $A\beta_{1-42}$.

The ability of Trolox to prevent the $A\beta_{1-42}$-induced changes in GLT-1 ubiquitination, membrane expression, detergent insolubility, and transport function suggests that oxidative stress is a relevant injury mechanism impairing the ability of hippocampal astrocytes to carry out their critical neuroprotective function.

Discussion

Our results show that $A\beta_{1-42}$ prolongs the lifetime of synaptically released glutamate at astrocytic membranes via oxidative stress, GLT-1 ubiquitination, and mislocalization at the cell membrane. These data support the notion that GLT-1 plays a key role in the pathogenesis of AD (Masliah et al., 1996; Lauderback et al., 2001; Jacob et al., 2007; Woltjer et al., 2010; Mookherjee et al., 2011) and suggest potential opportunities for therapeutic intervention. Notably, our results show that anti-oxidant pretreatment—not acute exposure—can prevent entirely the effects of $A\beta_{1-42}$ on GLT-1. Importantly, $A\beta_{1-42}$ treatment in acute slices recapitulates the aberrant GLT-1 detergent insolubility found in hippocampi of mildly cognitively impaired and late-stage AD patients (Woltjer et al., 2010).

The ability of $A\beta_{1-42}$ to double the amount of time it takes to clear synaptically released glutamate suggests that GLT-1 dysfunction may facilitate Aβ-related neurotoxicity. It also suggests that even under conditions where extracellular glutamate levels are restored to their normal baseline levels, $A\beta_{1-42}$ may still promote the spread of glutamate from one synaptic domain to another—an effect that could impair the normal activity of entire neuronal networks.

The effects of $A\beta_{1-42}$ on GLT-1 mislocalization, protein insolubility, and ubiquitination argue for the functional significance of rapidly occurring post-translational modifications of GLT-1 in AD-related pathogenesis. There is also evidence that longer-term exposure to $A\beta_{1-42}$ can cause GLT-1 loss in astrocytes that is mediated by numerous inflammation-related transcriptional processes (Abdul et al., 2009). GLAST levels are also reduced by inflammatory transcriptional processes (Sama et al., 2008). This may be related to why total glutamate transporter levels in our experiments trended lower, albeit nonsignificantly, due to short-term $A\beta_{1-42}$ exposure. Taken collectively, such findings and the data herein suggest that AD-related pathologic processes can disturb astrocytic glutamate transporters via multiple interrelated molecular pathways that ultimately lead to glutamate transporter loss in AD (Masliah et al., 1996; Jacob et al., 2007; Abdul et al., 2009; Woltjer et al., 2010).

The molecular mechanisms underlying the effect of $A\beta_{1-42}$ on GLT-1 therefore have important mechanistic implications for: (1) development of new treatments to combat oxidative stress in AD, like those pursued in ongoing clinical studies testing the efficacy of combining vitamin E and memantine, a drug thought to suppress excessive glutamate stimulation of the brain (ClinicalTrials.gov # NCT00235716); and (2) development of therapeutic strategies to limit the neurotoxicity of prolonged glutamate exposure/spread in AD (Lipton, 2005).

References

Abdul HM, Sama MA, Furman JL, Mathis DM, Beckett TL, Weidner AM, Patel ES, Baig I, Murphy MP, LeVine H 3rd, Kraner SD, Norris CM (2009) Cognitive decline in Alzheimer's disease is associated with selective changes in calcineurin/NFAT signaling. J Neurosci 29:12957–12969. CrossRef Medline

Chaudhry FA, Lehre KP, van Lookeren Campagne M, Ottersen OP, Danbolt NC, Storm-Mathisen J (1995) Glutamate transporters in glial plasma membranes: highly differentiated localizations revealed by quantitative ultrastructural immunocytochemistry. Neuron 15:711–720. CrossRef Medline

Diamond JS (2005) Deriving the glutamate clearance time course from transporter currents in CA1 hippocampal astrocytes: transmitter uptake gets faster during development. J Neurosci 25:2906–2916. CrossRef Medline

Diamond JS, Jahr CE (1997) Transporters buffer synaptically released glutamate on a submillisecond time scale. J Neurosci 17:4672–4687. Medline

Felipo V, Butterworth RF (2002) Neurobiology of ammonia. Prog Neurobiol 67:259–279. CrossRef Medline

Guo ZH, Mattson MP (2000) Neurotrophic factors protect cortical synaptic terminals against amyloid and oxidative stress-induced impairment of glucose transport, glutamate transport and mitochondrial function. Cereb Cortex 10:50–57. CrossRef Medline

Haugeto O, Ullensvang K, Levy LM, Chaudhry FA, Honoré T, Nielsen M, Lehre KP, Danbolt NC (1996) Brain glutamate transporter proteins form homomultimers. J Biol Chem 271:27715–27722. CrossRef Medline

Jacob CP, Koutsilieri E, Bartl J, Neuen-Jacob E, Arzberger T, Zander N, Ravid R, Roggendorf W, Riederer P, Grünblatt E (2007) Alterations in expression of glutamatergic transporters and receptors in sporadic Alzheimer's disease. J Alzheimers Dis 11:97–116. Medline

Kanai Y, Hediger MA (1992) Primary structure and functional characterization of a high-affinity glutamate transporter. Nature 360:467–471. CrossRef Medline

Lauderback CM, Hackett JM, Huang FF, Keller JN, Szweda LI, Markesbery WR, Butterfield DA (2001) The glial glutamate transporter, GLT-1, is oxidatively modified by 4-hydroxy-2-nonenal in the Alzheimer's disease brain: the role of Abeta1–42. J Neurochem 78:413–416. CrossRef Medline

Lipton SA (2005) The molecular basis of memantine action in Alzheimer's disease and other neurologic disorders: low-affinity, uncompetitive antagonism. Curr Alzheimer Res 2:155–165. CrossRef Medline

Martínez-Villarreal J, García Tardón N, Ibáñez I, Giménez C, Zafra F (2012) Cell surface turnover of the glutamate transporter GLT-1 is mediated by ubiquitination/deubiquitination. Glia 60:1356–1365. CrossRef Medline

Masliah E, Alford M, DeTeresa R, Mallory M, Hansen L (1996) Deficient glutamate transport is associated with neurodegeneration in Alzheimer's disease. Ann Neurol 40:759–766. CrossRef Medline

Mookherjee P, Green PS, Watson GS, Marques MA, Tanaka K, Meeker KD, Meabon JS, Li N, Zhu P, Olson VG, Cook DG (2011) GLT-1 loss accelerates cognitive deficit onset in an Alzheimer's disease animal model. J Alzheimers Dis 26:447–455. Medline

Quintanilla RA, Muñoz FJ, Metcalfe MJ, Hitschfeld M, Olivares G, Godoy JA, Inestrosa NC (2005) Trolox and 17beta-estradiol protect against amyloid beta-peptide neurotoxicity by a mechanism that involves modulation of the Wnt signaling pathway. J Biol Chem 280:11615–11625. CrossRef Medline

Sama MA, Mathis DM, Furman JL, Abdul HM, Artiushin IA, Kraner SD, Norris CM (2008) Interleukin-1beta-dependent signaling between as-

trocytes and neurons depends critically on astrocytic calcineurin/NFAT activity. J Biol Chem 283:21953–21964. CrossRef Medline

Scimemi A, Tian H, Diamond JS (2009) Neuronal transporters regulate glutamate clearance, NMDA receptor activation, and synaptic plasticity in the hippocampus. J Neurosci 29:14581–14595. CrossRef Medline

Stine WB Jr, Dahlgren KN, Krafft GA, LaDu MJ (2003) In vitro characterization of conditions for amyloid-beta peptide oligomerization and fibrillogenesis. J Biol Chem 278:11612–11622. CrossRef Medline

Sultana R, Boyd-Kimball D, Poon HF, Cai J, Pierce WM, Klein JB, Merchant M, Markesbery WR, Butterfield DA (2006) Redox proteomics identification of oxidized proteins in Alzheimer's disease hippocampus and cerebellum: an approach to understand pathological and biochemical alterations in AD. Neurobiol Aging 27:1564–1576. CrossRef Medline

Swanson RA, Liu J, Miller JW, Rothstein JD, Farrell K, Stein BA, Longuemare MC (1997) Neuronal regulation of glutamate transporter subtype expression in astrocytes. J Neurosci 17:932–940. Medline

Tanaka K, Watase K, Manabe T, Yamada K, Watanabe M, Takahashi K, Iwama H, Nishikawa T, Ichihara N, Kikuchi T, Okuyama S, Kawashima N, Hori S, Takimoto M, Wada K (1997) Epilepsy and exacerbation of brain injury in mice lacking the glutamate transporter GLT-1. Science 276:1699–1702. CrossRef Medline

Trotti D, Rizzini BL, Rossi D, Haugeto O, Racagni G, Danbolt NC, Volterra A (1997) Neuronal and glial glutamate transporters possess an SH-based redox regulatory mechanism. Eur J Neurosci 9:1236–1243. CrossRef Medline

Trotti D, Danbolt NC, Volterra A (1998) Glutamate transporters are oxidant-vulnerable: a molecular link between oxidative and excitotoxic neurodegeneration? Trends Pharmacol Sci 19:328–334. CrossRef Medline

Tsvetkov E, Shin RM, Bolshakov VY (2004) Glutamate uptake determines pathway specificity of long-term potentiation in the neural circuitry of fear conditioning. Neuron 41:139–151. CrossRef Medline

Voutsinos-Porche B, Bonvento G, Tanaka K, Steiner P, Welker E, Chatton JY, Magistretti PJ, Pellerin L (2003) Glial glutamate transporters mediate a functional metabolic crosstalk between neurons and astrocytes in the mouse developing cortex. Neuron 37:275–286. CrossRef Medline

Winer BJ, Brown DR, Michels KM (1991) Statistical principles in experimental design, Ed 3. New York: McGraw-Hill.

Woltjer RL, Cimino PJ, Boutté AM, Schantz AM, Montine KS, Larson EB, Bird T, Quinn JF, Zhang J, Montine TJ (2005) Proteomic determination of widespread detergent-insolubility including Abeta but not tau early in the pathogenesis of Alzheimer's disease. FASEB J 19:1923–1925. Medline

Woltjer RL, Duerson K, Fullmer JM, Mookherjee P, Ryan AM, Montine TJ, Kaye JA, Quinn JF, Silbert L, Erten-Lyons D, Leverenz JB, Bird TD, Pow DV, Tanaka K, Watson GS, Cook DG (2010) Aberrant detergent-insoluble excitatory amino acid transporter 2 accumulates in Alzheimer disease. J Neuropathol Exp Neurol 69:667–676. CrossRef Medline